

*X-rays at Sharp Focus: Chandra Science Symposium
ASP Conference Series, Vol. **VOLUME**, 2002
eds. S. Vrtilek, E. M. Schlegel, L. Kuhi*

The Low-Energy Spectral Response of the ACIS CCDs

Paul P. Plucinsky, Richard J. Edgar and Shanil N. Virani

*Harvard-Smithsonian Center for Astrophysics, 60 Garden St., MS-70,
Cambridge, MA 02138*

Leisa K. Townsley and Patrick S. Broos

*Department of Astronomy & Astrophysics, The Pennsylvania State
University, 525 Davey Lab, University Park, PA 16802*

Abstract. The flight calibration of the spectral response of the *Advanced CCD Imaging Spectrometer* (ACIS) below 1.5 keV is difficult because of the lack of strong lines in the calibration source on-board the *Chandra X-ray Observatory*. We have been using 1E0102.2-7219 (the brightest supernova remnant in the SMC) to evaluate the ACIS response matrices, since this remnant has strong lines of O, Ne and Mg below 1.5 keV. The spectrum of 1E0102.2-7219 has been well-characterized using the gratings on *Chandra* and *XMM*. We have used the high-resolution spectral data from both gratings instruments to develop a spectral model for the CCD spectra. Fits with this model are sensitive to any problems with the gain calibration and the spectral redistribution model. We have fit the data with the latest response matrix for the S3 device released in August 2001 (available in CALDB 2.7 or higher). We have also applied the charge-transfer inefficiency (CTI) correction software (version 1.37) developed at Penn State to both the Backside-illuminated (BI) and Front-side illuminated (FI) data and fit the data with the associated CTI-corrected response matrices. All fits show a significant improvement in the low energy response with the new matrices. The fits to the FI CCDs demonstrate the utility of the FI CCDs for spectral analysis, in spite of the radiation damage the devices suffered early in the mission.

1. Introduction

The *Advanced CCD Imaging Spectrometer* (ACIS) instrument team, at both Penn State and MIT, and the Chandra X-ray Center (CXC) have been working to improve the quality of the flight calibration of the ACIS CCDs. The CXC has recently released a new response matrix for the S3 CCD at -120 C in the CALDB 2.7 and CIAO 2.1.3 release (see asc.harvard.edu/cal/Links/Acis/acis/Cal_prods/matrix/matrix.html). The new matrix includes a more sophisticated representation of the spectral redistribution function and an improved model of the gain at energies below 1 keV. The major difference between the CALDB 2.7 matrices and previous matrices is at energies below 1 keV, with little or no difference at energies above 1.5 keV. There has been no change to the quantum efficiency model of the detector.

The ACIS instrument team has released software (SW) to correct for the charge-transfer inefficiency (CTI) of both the Frontside-illuminated (FI) and Backside-illuminated (BI) CCDs. The physical model of the CCD is described in Townsley *et al.* (2001a) and the details of the CTI correction are given in Townsley *et al.* (2000) and Townsley *et al.* (2001b). The CTI correction SW (version 1.37) and accompanying response matrices (30JUL01) are available at “www.astro.psu.edu/users/townsley/cti/” or from the contributed SW page at the CXC web site “asc.harvard.edu/cgi-gen/cont-soft/soft-list.cgi”. The CTI correction for the BI CCD is small but is rather large for the FI CCDs, and makes a dramatic difference in spectral fits with the FI CCDs.

In this paper, we will focus on the low energy response as described by the response matrices listed above. Specifically, we will use strong lines in the spectrum of the bright, SMC supernova remnant (SNR) 1E0102.2-7219 in the region between 0.5-1.5 keV to test the new response matrices. The spectrum of 1E0102.2-7219 has been well-characterized using the gratings on *XMM* (see Rasmussen *et al.* 2001 and Sasaki *et al.* 2001) and also on *Chandra* (see Canizares *et al.* 2001, Flanagan *et al.* 2001, and Davis *et al.* 2001). The spectrum is dominated by strong lines from O VII, O VIII, Ne IX, Ne X, Mg XI, and Mg XII. The high resolution gratings spectra show that there is little or no Fe emission in this spectrum. The lack of Fe in the 1E0102.2-7219 spectrum greatly simplifies the modeling of the spectrum, since the Ne lines are not blended with the Fe L lines.

2. Data

We used six datasets for the S3(BI) analysis and five datasets for the I3(FI) analysis. The datasets are listed in Table 1 with the date of observation, position on the CCD, and exposure time. The six datasets for S3 sample four regions on the CCD, since two of the observations were executed at the same location on the chip but at different times to check for temporally-varying performance. The five datasets on I3 sampled five different locations in row number on the CCD in order to characterize the effect of CTI on low-energy X-rays. All of these observations are calibration observations and are available in the *Chandra* public archive.

The spectra were extracted and response matrices and auxiliary response files generated using the standard *CIAO* tools `dmextract`, `mkrmf`, `mkarf` using *CIAO* 2.1.3 and CALDB 2.7 for the S3 data. For the I3 data and also for the S3 dataset OBSID 1311, the spectra were extracted using `dmextract` but specifying the binning of PI channels described in the recipe on the CTI correction SW page. The different channel types are labeled in Figure 1 as “PHA” and “PI” for the channel types produced by the *CIAO* SW and “PPI” for the channel types produced by the Penn State CTI-correction SW. We used the response matrices for I3 and S3 appropriate for CTI-corrected data based on the position of the source on the chip (see the CTI-correction web pages for more details). We used an annulus for the spatial extraction region in order to maximize the contribution of the shocked ejecta and to minimize the contribution of the primary blastwave of the remnant (see Hughes *et al.* 2001 and Gaetz *et al.* 2001). Extracting spectra from this annulus should maximize the contrast between the lines and the underlying continuum.

Table 1. List of 1E0102.2-7219 Observations Used

OBSID	DATE	y-offset (arcmin)	z-offset (arcmin)	CCD column	CCD row	Exp (ks)
BI(S3) Datasets						
1311	2000-12-10	-1.0	0.0	374	506	7.8
1531	2001-06-06	-1.0	0.0	362	507	7.5
1308	2000-12-10	1.0	0.0	130	508	8.0
1530	2001-06-06	1.0	0.0	116	508	7.7
141	2000-05-28	-1.0	2.0	364	262	9.8
1702	2000-05-28	-1.0	-2.0	366	752	9.6
FI(I3) Datasets						
440	2000-04-04	-0.5	2.5	662	904	6.9
439	2000-04-04	-2.25	2.5	662	690	6.9
136	2000-03-16	-4.0	2.5	661	476	10.0
140	2000-04-04	-5.5	2.5	662	291	8.3
420	2000-03-14	-7.0	2.5	658	104	10.2

3. Spectral Analysis

3.1. Spectral Model

We developed a spectral model (based on the high-resolution gratings data) which consisted of two components for absorption (one for the galactic contribution and one for the SMC contribution with variable abundances), a bremsstrahlung component for the continuum, and Gaussians for the lines. The energies of the Gaussians were set to their known values and not allowed to vary during the fitting process. The widths of the lines were set to zero, so that the width is completely determined by the spectral redistribution function of the matrix. The HETG data indicate that there are measurable Doppler shifts in these lines on the order of a few eV, but these are small compared to the resolution of the detector ($\sim 75 - 150$ eV). Only the normalizations of the lines were allowed to vary. In this manner, this model was used to verify that the lines were modeled at the correct energy in the matrices and the shapes of the lines were consistent with the widths contained in the matrices. Our model contains a total of 24 lines determined from the gratings spectra, but in most of the fits three or four of the lines are fitted with a zero normalization.

3.2. S3(BI) Spectral Fits

The spectral model described above was fit to all of the datasets in Table 1. The values of the reduced χ^2 ranged from 1.1 to 2.1. Table 2 and Figure 1 summarize the fitted values for the N_{H} and kT . OBSID 1311 was fitted in both PHA and PI channel space with the CALDB 2.7 matrices and the resulting values agreed well with each other. OBSID 1311 was also fitted after applying the CTI correction. The fitted value of kT was consistent with the value derived from the CXC matrix fits, but the fitted value of the N_{H} was discrepant at the 90% confidence limit (CL). OBSIDs 1531, 1308, 1530, 141, and 1702 were fitted in PHA space and compared to OBSID 1311. All datasets agreed within the 90% CL except for OBSID 1530. OBSID 1308 agreed within the 90% CL, but had the largest

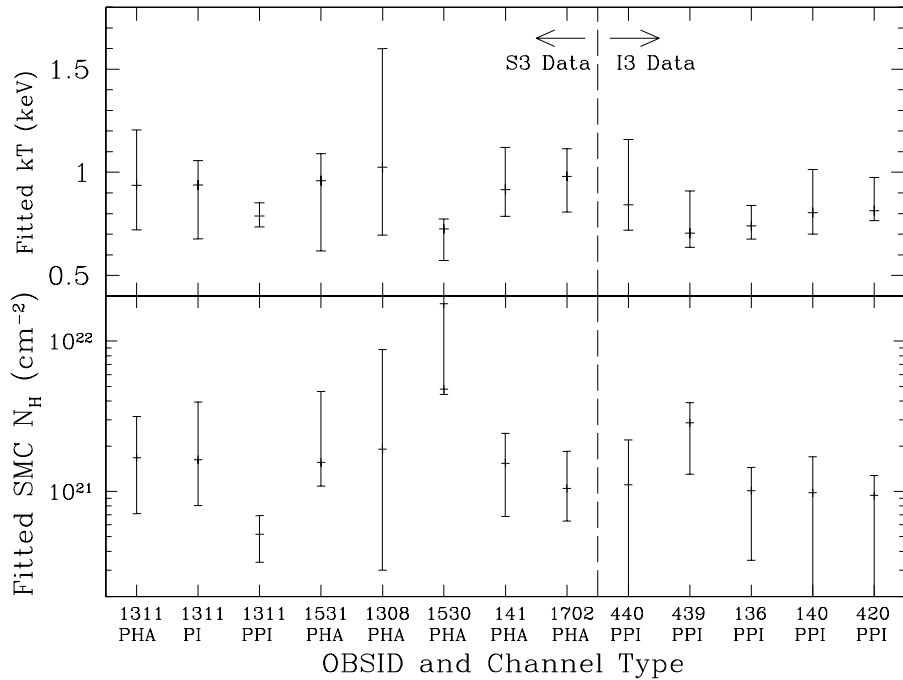


Figure 1. Fitted Values vs OBSIDs for S3(BI) and I3(FI). The channel types “PHA” and “PI” refer to channels produced by the *CIAO* SW and “PPI” refers to channels produced by the Penn State CTI correction SW. Error bars are 90% CL.

error bars by far of any dataset. Both OBSID 1530 and 1308 warrant further investigation for instrumental effects which may have compromised the data.

Figure 2 displays the fit to OBSID 1311 in PHA space. The matrix and model represent the data extremely well from 700 eV to 1600 eV. Note how well the Ne lines at ~ 900 eV and ~ 1000 eV are fitted by this matrix and model. There are data from 1.6 keV to 5.0 keV which we have chosen to exclude from the plot since there are no strong lines in that region, but which are included in the fit. Only below 700 eV is there any evidence of systematic effects in the residuals. The fits to the other data sets and to the CTI-corrected data are qualitatively similar. These data confirm that the CALDB 2.7 matrix has correctly incorporated the gain and spectral redistribution function of the BI(S3) CCD and that data from four different locations on the S3 detector produce similar fitted results.

3.3. I3(FI) Spectral Fits

We fit the five datasets on the I3 CCD which span the regions from low row numbers where the CTI effects are minimized to high row numbers where the CTI effects are largest. The results are summarized for OBSIDs 440, 439, 136, 140, and 420 in Table 2 and Figure 1. The fitted values for the N_H and kT are all consistent with each other at the 90% CL, except for the N_H for OBSIDs 420 and

Table 2. Spectral Fit Results with 90% Confidence Limits

OBSID	SMC N_{H} (10^{21} cm^{-2})	kT (keV)	Red χ^2	DOF
BI(S3) Datasets				
1311	1.68 [0.71,3.15]	0.94 [0.72,1.21]	1.46	117
1311	1.63 [0.80,3.94]	0.94 [0.68,1.06]	1.73	78 (CXC PI)
1311	0.52 [0.34,0.69]	0.79 [0.74,0.85]	1.35	80 (PSU PI)
1531	1.56 [1.08,4.63]	0.96 [0.62,1.09]	1.31	111
1308	1.91 [0.30,8.80]	1.03 [0.70,1.60]	2.06	121
1530	4.80 [4.43,17.8]	0.73 [0.57,0.77]	1.46	118
141	1.54 [0.68,2.43]	0.92 [0.79,1.12]	1.68	125
1702	1.05 [0.64,1.85]	0.98 [0.81,1.11]	1.17	125
FI(I3) Datasets, CTI-Corrected, PSU matrix				
440	1.11 [0.10,2.20]	0.84 [0.72,1.16]	1.28	59
439	2.86 [1.30,3.90]	0.71 [0.64,0.91]	1.08	61
136	1.01 [0.35,1.44]	0.74 [0.68,0.84]	1.52	63
140	0.98 [0.00,1.71]	0.80 [0.70,1.10]	1.74	58
420	0.94 [0.00,1.26]	0.81 [0.77,0.98]	1.89	60

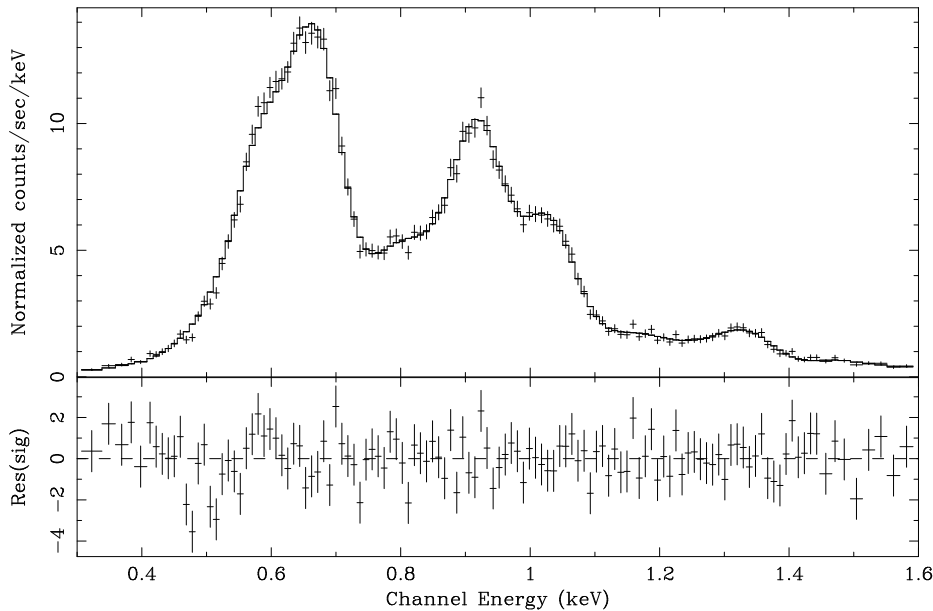


Figure 2. OBSID 1311: Fit with the CXC CALDB 2.7 S3 matrix in PHA space.

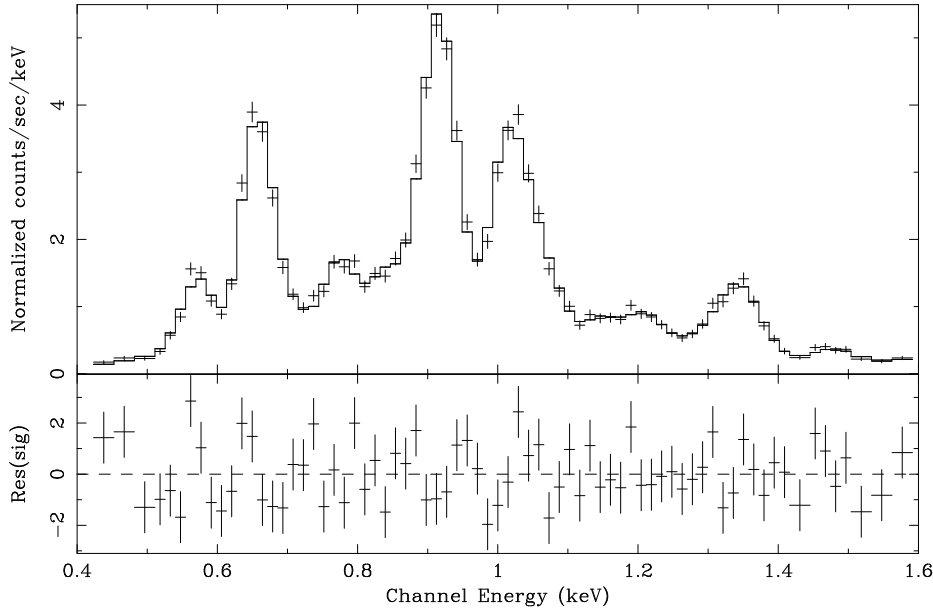


Figure 3. OBSID 420: Fit with the PSU 30JUL01 matrix in PI space (row=104).

439. The consistency of the fitted results demonstrates the value and accuracy of the CTI correction. The spectra for OBSIDs 420, 136, and 440 are shown in Figures 3, 4, and 5. The quality of the fits is good with the reduced χ^2 values ranging from 1.1 to 1.9. Only around 650 eV is there any evidence of systematic effects in the residuals. It is clear from these plots that the spectral resolution of the detector changes dramatically with row number. The gain of the detectors is also changing, but this effect has also been corrected by the CTI correction SW. The data from OBSID 420 show that the spectral resolution of I3 at low row numbers is significantly better than S3 (see Virani *et al.* these proceedings). Note how cleanly the O and Ne lines are separated in Figure 3 and compare to the S3 spectrum in Figure 2. In fact, OBSID 136 shows that I3 has better spectral resolution than S3 halfway across the CCD. It is only in the top half of the FI CCDs where the resolution is worse than S3 after correcting for CTI as shown in Figure 5.

4. Conclusions

We have used the soft, line-dominated spectrum of the SMC SNR 1E0102.2-7219 to evaluate the response matrices of the BI and FI CCDs at low energies. We have demonstrated that the new BI(S3) matrices released in August 2001 in CALDB 2.7 and in the Penn State CTI correction SW are an accurate representation of the spectral response of the S3 CCD from 0.7 to 1.6 keV. We have used several datasets of 1E0102.2-7219 on S3 to verify that the new matrix

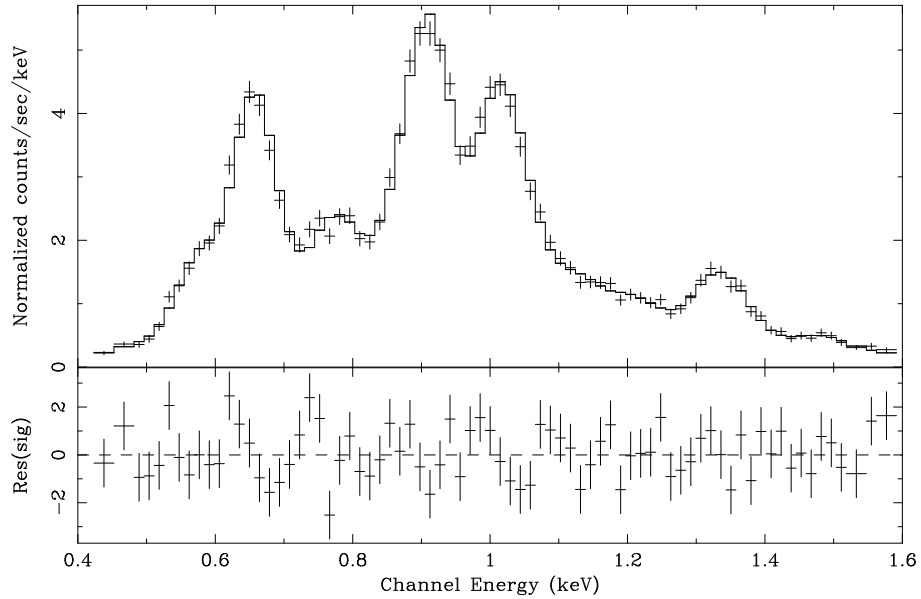


Figure 4. OBSID 136: Fit with the PSU 30JUL01 matrix in PI space (row=476).

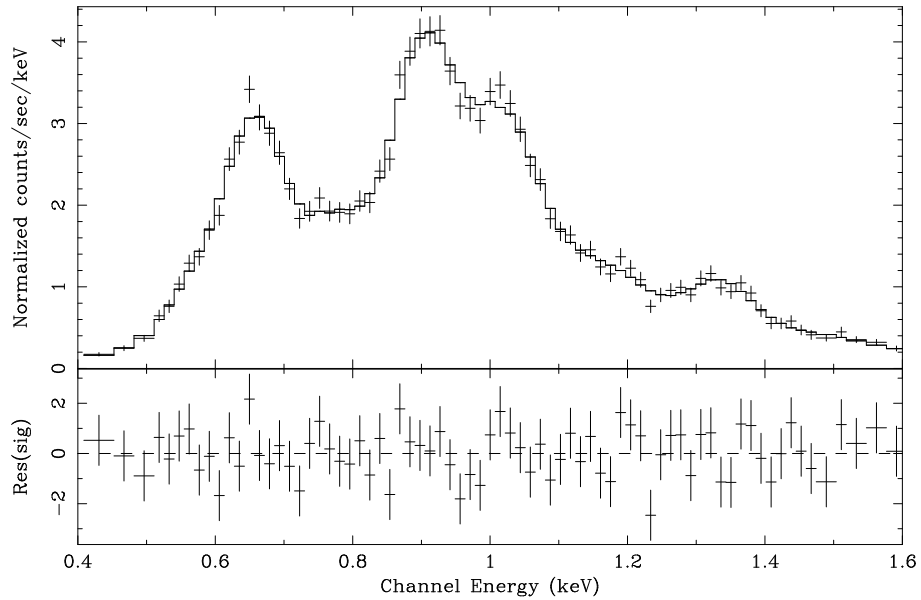


Figure 5. OBSID 440: Fit with the PSU 30JUL01 matrix in PI space (row=904).

yields consistent fitted parameters for different locations on the CCD. We have applied the Penn State CTI correction SW to five datasets on the I3(FI) CCD and demonstrated that the SW corrects for the spatial dependence of the gain and the spatial dependence of the redistribution function due to CTI. The fits indicate that the response matrix is an accurate representation of the spectral response of the I3 CCD. We derive fitted parameters which are consistent with each other at the 90% CL, even though the spectral resolution of the I3 CCD is changing rapidly with position. In fact, after CTI correction the FI CCDs have superior spectral resolution compared to S3 across the bottom half of the CCDs. *Chandra* observers should be aware of this performance and use it to their advantage if possible.

5. Acknowledgments

We thank all of our colleagues at the CXC, PSU, and MIT who have helped with the flight calibration of the ACIS instrument. We thank all of the engineers, technicians, and scientists who have made the *Chandra X-ray Observatory* such a success. PPP, RJE, and SNV acknowledge support for this work from NASA contract NAS8-39703. LKT and PSB acknowledge support for this work from NASA contract NAS8-38252.

References

Canizares, C.R., Flanagan, K.A., Davis, D.S., Dewey, D., Houck, J.C., Schattenburg, M.L. 2001, in "Young Supernova Remnants" (11th Astrophysics Conference in Maryland), S. S. Holt & U. Hwang (eds), AIP, New York (2001)

Davis, D.S., Flanagan, K.A., Houck, J.C., Canizares, C.R., Allen, G.E., Schulz, N.S., Dewey, D., Schattenburg, M.L. 2001, in "Young Supernova Remnants" (11th Astrophysics Conference in Maryland), S. S. Holt & U. Hwang (eds), AIP, New York (2001)

Flanagan, K.A., Canizares, C.R., Davis, D.S., Dewey, D., Houck, J.C., Markert, T.H., Schattenburg, M.L. 2001, in the ASP Conference Series for X-ray Astronomy 2000, Palermo Italy, eds. Giacconi, Stella & Serio

Gaetz, T. J., Butt, Y. M., Edgar, R. J., Eriksen, K. A., Plucinsky, P. P., Schlegel, E. M., & Smith, R. K. 2000, ApJL, 534, L47

Hughes, J. P., Rakowski, C. E., & Decourchelle, A. 2000, ApJL, 543, L61

Rasmussen, A. P., Behar, E., Kahn, S. M., den Herder, J. W., & van der Heyden, K. 2001, A&A, 365, L231

Sasaki, M., Stadlbauer, T. F. X., Haberl, F., Filipović, M. D., & Bennie, P. J. 2001, A&A, 365, L237

Townsley, L. K., Broos, P. S., Garmire, G. P., & Nousek, J. A. 2000, ApJL, 534, L139

Townsley, L. K., Broos, P. S., Chartas, G., Moskalenko, E., Nousek, J.A., & Pavlov, G.G., 2001, NIM, accepted, A

Townsley, L. K., Broos, P. S., Nousek, J.A., & Garmire, G.P., 2001, NIM, accepted, B

Virani, S.N., Plucinsky, P.P., Grant, C.E., & LaMarr, B. 2001, these proceedings